Supporting Information

Ti-doped Iron Phosphide Nanoarrays Grown on Carbon Cloth as a Self-supported Electrode for Enhanced Electrocatalytic Nitrogen Reduction

Senhao Wang,[a] Yuan Wang,[a]* Tian C. Zhang,[b] Xu Ji,[a] Shaojun Yuan[a]*

[a] Low-carbon Technology & Chemical Reaction Engineering Lab, College of Chemical Engineering, Sichuan University, Chengdu 610065, P. R. China
[b] Civil & Environmental Engineering Department, University of Nebraska-Lincoln, Omaha, NE 68182-0178, USA
*Corresponding author: E-mail: wangyuan2022@scu.edu.cn (Y. Wang), ysj@scu.edu.cn (S.J. Yuan), Tel/fax: +86-28-85405201

S1. Supplementary Experimental

S1.1. Determination of NH$_3$

The yield of NH$_3$ production was determined by the indophenol blue method. 50 μL oxidizing solution (4.5% NaClO and 0.75 M NaOH), 500 μL coloring solution (0.32 M NaOH and 0.4 M C$_7$H$_5$NaO$_3$), and 50 μL catalytic solution (10 g L^{-1} C$_5$FeN$_6$Na$_2$O·2H$_2$O) are added sequentially to the 4 mL tested electrolyte. The mixed solution is placed in the dark for 1 h, then determines the characteristic peak at 660 nm by an UV-vis spectrophotometer (UV-TU1810PC, Meishi Instrument, China). The fitted standard curve (y = 0.486x + 0.030, R^2 = 0.999) obtained by performing absorbance tests on NH$_4$Cl solutions with different concentrations shows a good linear relationship between the absorbance and concentration of NH$_3$.

S1.2. Determination of N$_2$H$_4$

The possible by-product N$_2$H$_4$ during the NRR electro-reduction was performed by the Watt and Chrisp method. The coloring solution is prepared by C$_9$H$_{11}$NO (5.99 g), concentrated HCl (30 mL) and C$_2$H$_5$OH (300 mL). Add 1 mL the above solution to 1 mL tested electrolyte.

The mixed solution is placed for 15 min, then determines the characteristic peak at 455 nm by an UV-vis spectrophotometer. The fitted standard curve ($y = 0.816x + 0.018$, $R^2 = 0.999$) obtained by performing absorbance tests on N_2H_4 solutions of different concentrations shows a good linear relationship between the absorbance and concentration of N_2H_4.
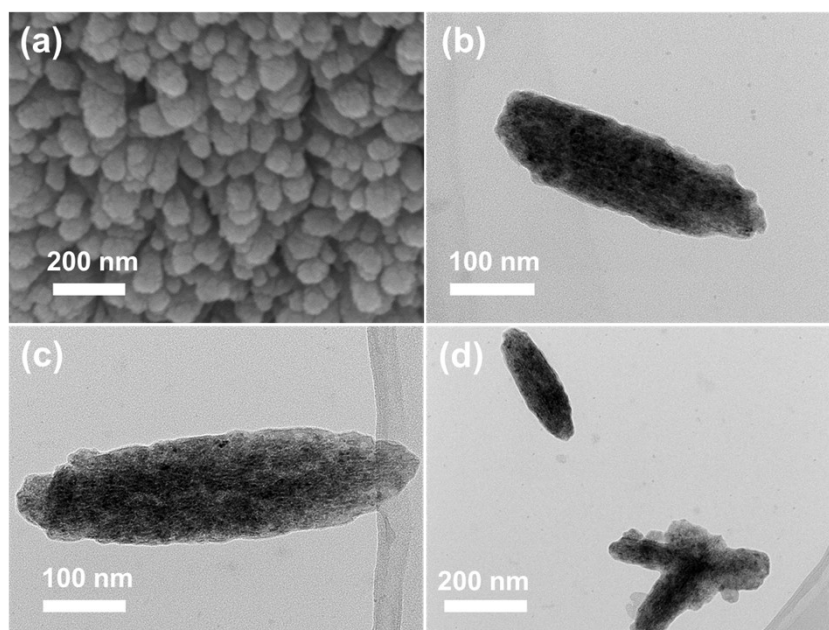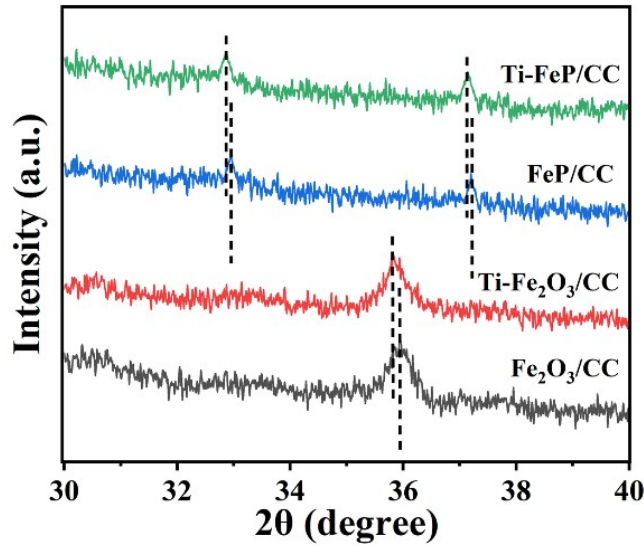

Fig. S1. (a) SEM image of Ti-FeP/CC at higher magnification. (b-d) TEM images of nanorod Ti-FeP/CC.
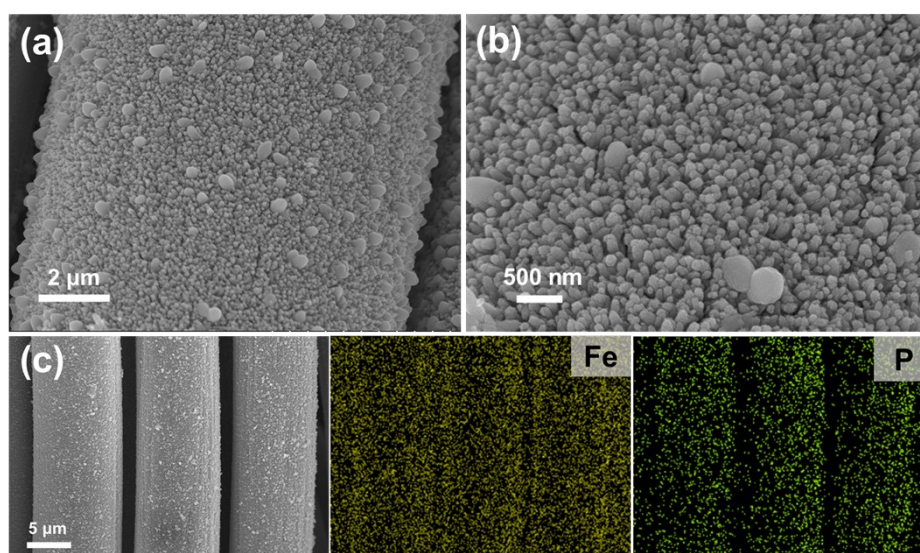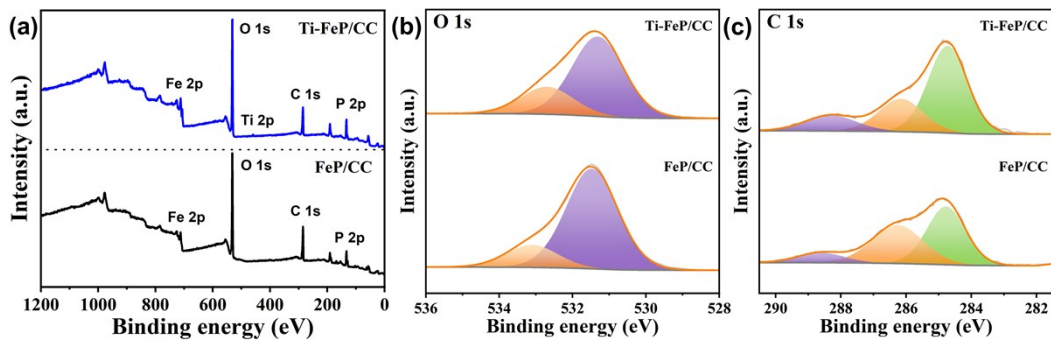

Fig. S2. (a and b) SEM images of FeP/CC. (c) SEM image and corresponding EDX elemental mapping images of FeP/CC.
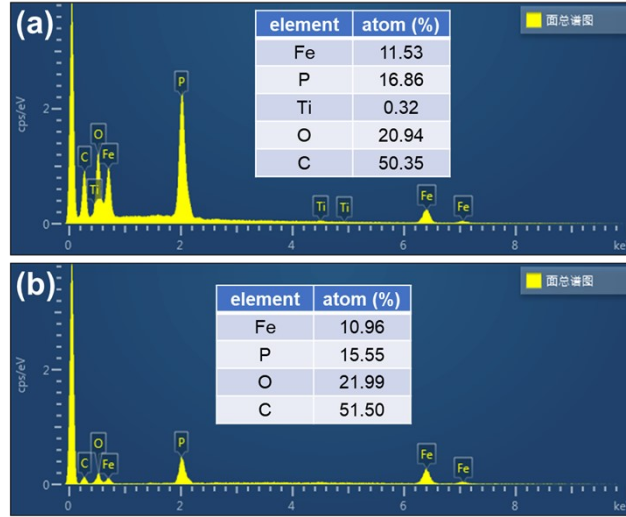
**Fig. S3.** EDX spectrum of Ti-FeP/CC (a) and FeP/CC (b).

Fig. S4. The magnified XRD patterns of Fe_2O_3/CC, Ti-Fe_2O_3/CC, FeP/CC and Ti-FeP/CC ranged from 30° to 40°.


Fig. S5. (a) XPS survey spectra of Ti-FeP/CC and FeP/CC. High resolution XPS spectra of Ti-FeP/CC: (b) O 1s; and (c) C 1s.

Table S1. Solution resistance (R_s) and charge transfer resistance (R_{ct}) of Ti-FeP/CC and FeP/CC determined by EIS spectra.

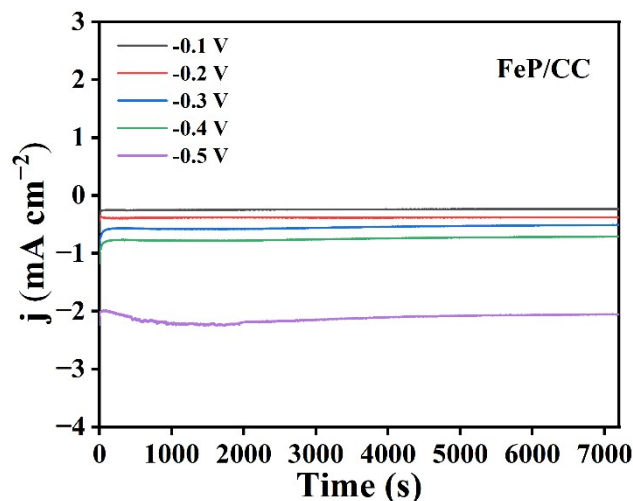| Catalyst	R_s (ohm)	R_{ct} (ohm)	Equivalent circuit diagram
Ti-FeP/CC	11.065	**0.06405**	
FeP/CC	11.114	0.09486	
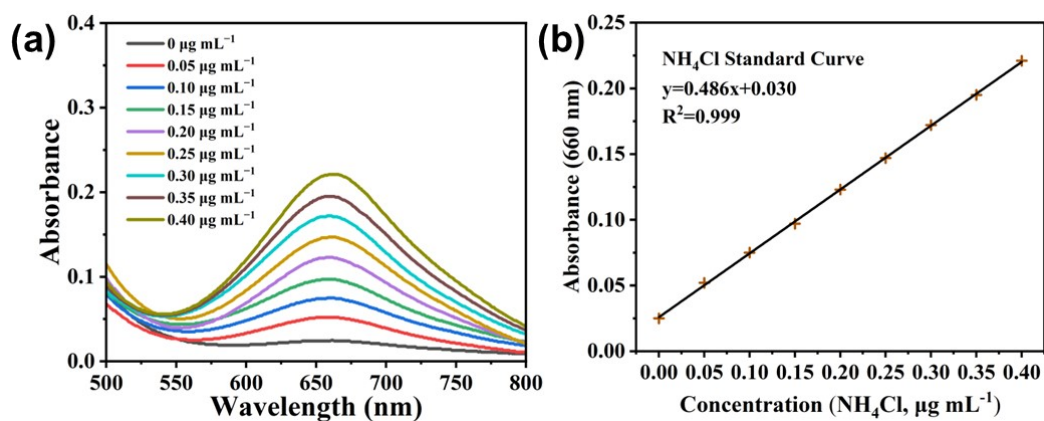
Fig. S6. (a) UV-vis spectra of various NH_4^+ concentrations. (b) Calibration curve used for calculation of NH_3 concentrations.
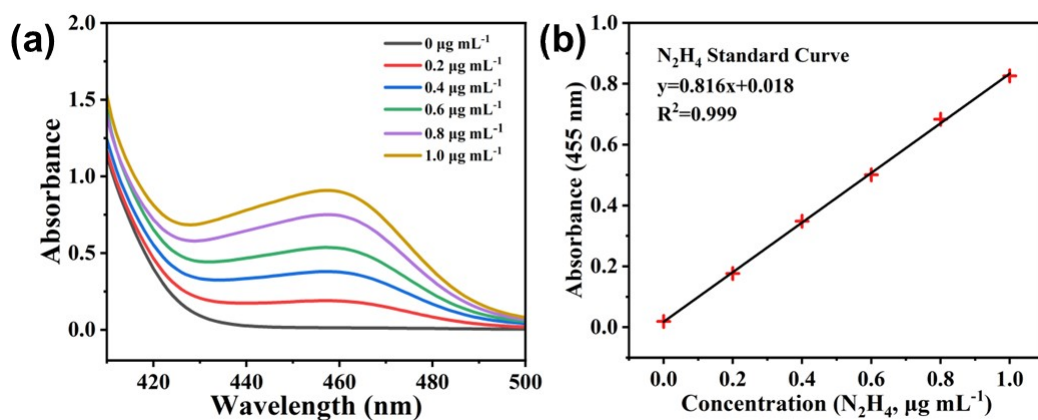
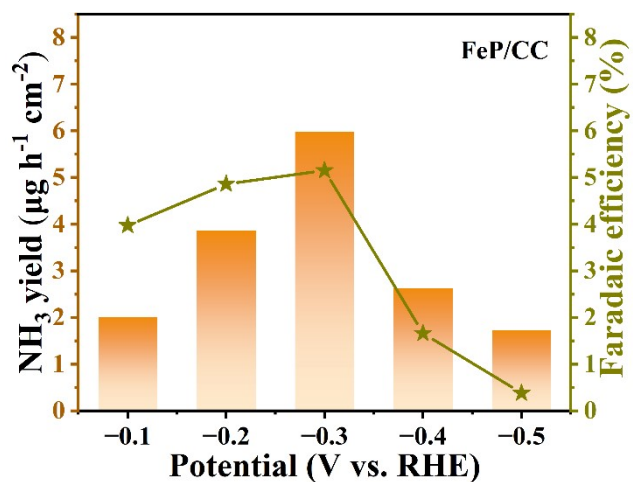**Fig. S7.** UV-vis spectra of various N_2H_4 concentrations. (b) Calibration curve used for calculation of N_2H_4 concentrations.
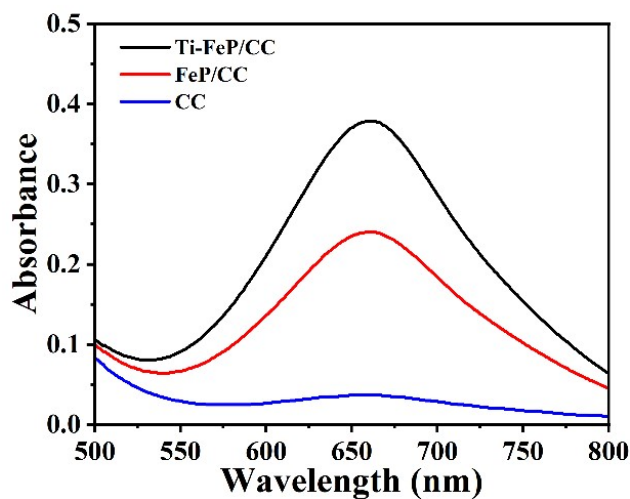
Fig. S8. Chronoamperometry curves of FeP/CC in N_2-saturated 0.1 M Na_2SO_4 solution at different potentials for 2 h.
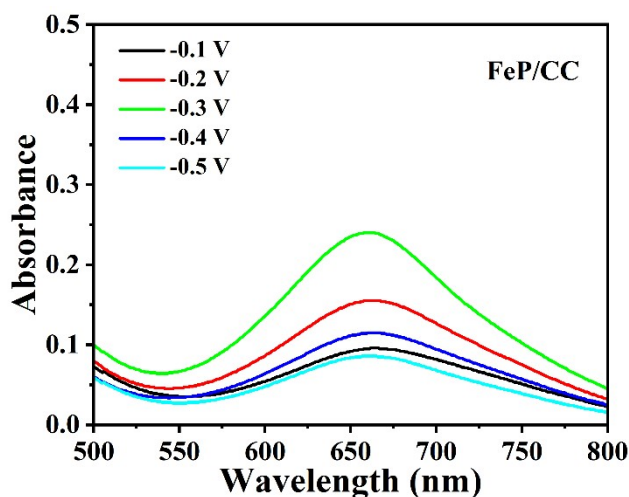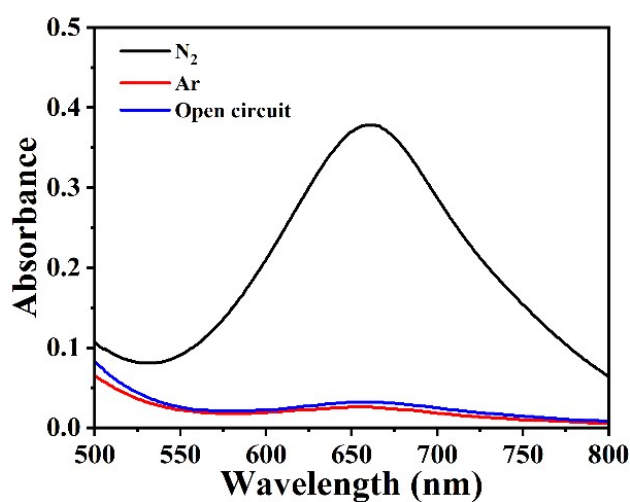

Fig. S9. UV-vis absorption spectra of electrolytes obtained by FeP/CC at different potentials stained with the indophenol indicator.
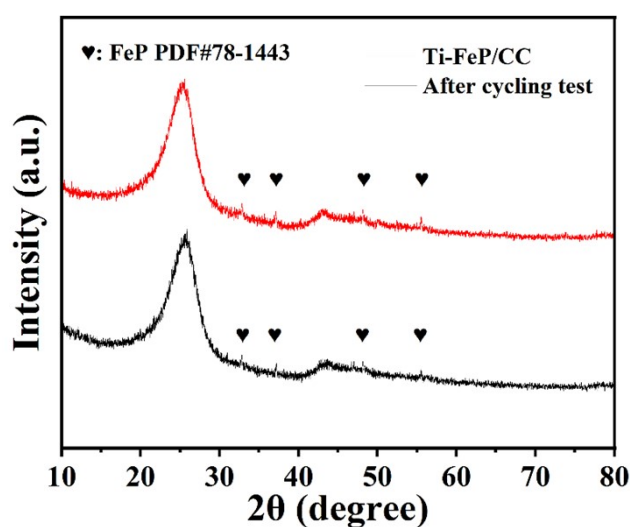

Fig. S10. NH_3 yield and Faradaic efficiency of FeP/CC at corresponding potentials.

Fig. S11. UV-vis absorption spectra of NH_4^+ on different electrodes at -0.30 V after 2 h electrolysis.

Fig. S12. UV-vis absorption spectra of NH_4^+ on Ti-FeP/CC at different potentials after electrolysis for 2 h under different electrochemical conditions.

Fig. S13. XRD patterns of the Ti-FeP/CC electrode after NRR stability measurement.
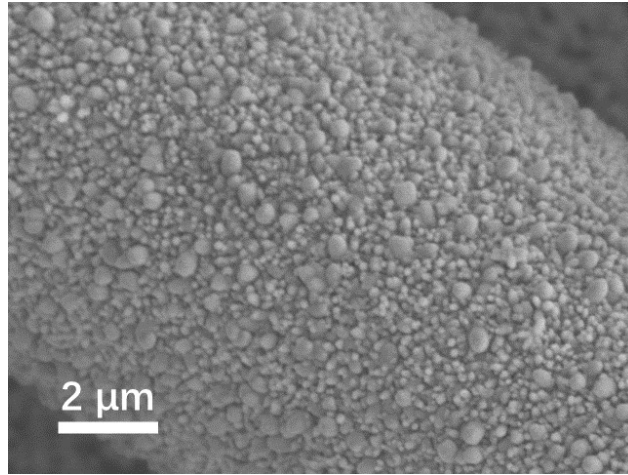
Fig. S14. SEM image of the Ti-FeP/CC after NRR stability measurement.

Fig. S15. Long-term current density time curve at -0.3 V (vs. RHE) for 48 h.

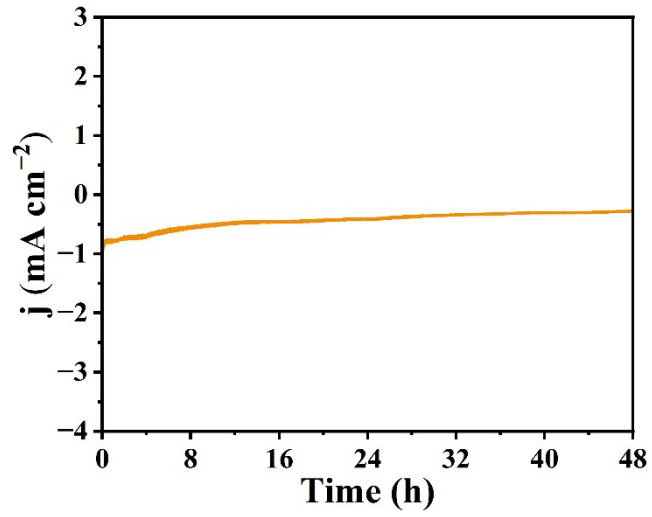**Table S2**. Comparison of NRR performance of previously reported transition metal-based catalysts.

Catalyst	Electrolyte	NH$_3$ yield	FE (%)	Ref.
Ti-FeP/CC	**0.1 M Na$_2$SO$_4$**	**10.93 μg h^{-1} cm^{-2}** **(1.79×10^{-10} mol s^{-1} cm^{-1})**	**10.77**	**This Work**
FeS@MoS$_2$	0.1 M HCl	8.45 μg h^{-1} cm^{-2}	2.96	1
NH$_2$-MIL-88B-Fe	0.1 M Na$_2$SO$_4$	1.205×10^{-10} mol s^{-1} cm^{-1}	12.45	2
CoFe$_2$O$_4$	0.1 M Na$_2$SO$_4$	4.22×10^{-11} mol s^{-1} cm^{-1}	6.2	3
MoN NA	0.1 M HCl	3.01×10^{-10} mol s^{-1} cm^{-1}	1.15	4
TiO$_2$/Ti	0.1 M Na$_2$SO$_4$	9.16×10^{-11} mol s^{-1} cm^{-1}	2.50	5
Al-Co$_3$O$_4$	0.1 M KOH	6.48×10^{-11} mol s^{-1} cm^{-1}	6.25	6
PdRu NS-NF	0.1 M KOH	20.46 μg h^{-1} cm^{-2}	2.11	7
VN/TM	0.1 M HCl	8.40×10^{-11} mol s^{-1} cm^{-1}	2.25	8
Fe$_2$O$_3$-CNT	KHCO$_3$	2.2×10^{-3} μg h^{-1} cm^{-2}	0.03	9
CuO/RGO	0.1 M Na$_2$SO$_4$	1.8×10^{-10} mol s^{-1} cm^{-1}	3.9	10

References

1. Y. Guo, Z. Yao, B. J. J. Timmer, X. Sheng, L. Fan, Y. Li, F. Zhang and L. Sun, *Nano Energy*, 2019, **62**, 282-288.
2. X. Yi, X. He, F. Yin, T. Yang, B. Chen and G. Li, *J. Mater. Sci.*, 2020, **55**, 12041-12052.
3. M. I. Ahmed, S. Chen, W. Ren, X. Chen and C. Zhao, *Chem. Commun.*, 2019, **55**, 12184-12187.
4. L. Zhang, X. Ji, X. Ren, Y. Luo, X. Shi, A. M. Asiri, B. Zheng and X. Sun, *ACS Sustain. Chem. Eng.*, 2018, **6**, 9550-9554.
5. R. Zhang, X. Ren, X. Shi, F. Xie, B. Zheng, X. Guo and X. Sun, *ACS Appl. Mater. Interfaces*, 2018, **10**, 28251-28255.
6. X.-W. Lv, Y. Liu, R. Hao, W. Tian and Z.-Y. Yuan, *ACS Appl. Mater. Interfaces*, 2020, **12**, 17502-17508.
7. Y. Li, H. Yu, Z. Wang, S. Liu, Y. Xu, X. Li, L. Wang and H. Wang, *Int. J. Hydrogen Energy*, 2020, **45**, 5997-6005.
8. R. Zhang, Y. Zhang, X. Ren, G. Cui, A. M. Asiri, B. Zheng and X. Sun, *ACS Sustain. Chem. Eng.*, 2018, **6**, 9545-9549.
9. S. Chen, S. Perathoner, C. Ampelli, C. Mebrahtu, D. Su and G. Centi, *Angew. Chem., Int. Ed.*, 2017, **56**, 2699-2703.
10. F. Wang, Y.-p. Liu, H. Zhang and K. Chu, ChemCatChem, 2019, 11, 1441-1447.